ChemComm

COMMUNICATION

View Article Online
View Journal | View Issue

Cite this: *Chem. Commun.*, 2020, **56**, 11122

Received 24th April 2020,
Accepted 9th July 2020

DOI: 10.1039/d0cc02988b

rsc.li/chemcomm

Detecting protein–protein interactions by Xe-129 NMR†

Zhuangyu Zhao, Benjamin W. Roose, Serge D. Zemerov, Madison A. Stringer and Ivan J. Dmochowski *

Detection of protein–protein interactions (PPIs) is limited by current bioanalytical methods. A protein complementation assay (PCA), split TEM-1 β-lactamase, interacts with xenon at the interface of the TEM-1 fragments. Reconstitution of TEM-1—promoted here by cFos/cJun leucine zipper interaction—gives rise to sensitive ^{129}Xe NMR signal in bacterial cells.

The analysis of protein–protein interactions (PPIs) is crucial for understanding protein functions and cell physiology. The protein complementation assay (PCA) is widely used for *in vivo* detection and validation of PPIs, whereby two catalytically or spectroscopically inactive halves of a reporter protein, *e.g.*, β-lactamase, green fluorescent protein (GFP), or luciferase, are fused to a pair of potentially interacting proteins.[1–9] The PPI reconstitutes the functional reporter, which gives a detectable readout such as enzymatic activity, fluorescence, or bioluminescence.[3–5,10–12] While enzymatic activity can be readily monitored by cell resistance to addition of antibiotics or deprivation of nutrient, and is thus useful for high-throughput screening, it is less suitable for obtaining spatiotemporal information. Previous studies mostly relied on fluorescence and luminescence to probe dynamic PPIs.[13–20] These imaging techniques are successfully applied to biochemical studies in cell lines and small, transparent model organisms.[5,6,14,21] However, optical approaches have limitations introduced by non-specific protein binding, endogenous fluorescence quenchers, and varying intracellular environments, such as pH and oxygenation, which can affect quantum yield and rates of photobleaching. New analytical methods for studying PPIs are needed, particularly to enable *in vivo* studies.

Nuclear magnetic resonance (NMR) spectroscopic techniques have evolved as useful tools to monitor PPIs that are difficult to study by other methods, and provide structural details of the protein interfaces.[22–30] However, NMR experiments using ^{1}H, ^{13}C and ^{15}N nuclei often suffer from low sensitivity, especially for medium to large protein systems, poor selectivity due to complicated biological environments, and usually require isotopic labelling. ^{129}Xe NMR can provide good selectivity due to low intrinsic background signal and excellent detection sensitivity owing to hyperpolarized (hp) ^{129}Xe chemical exchange saturation transfer (hyper-CEST).[31] This NMR technique applies selective saturation pulses at the ^{129}Xe-host chemical shift and monitors depolarization of ^{129}Xe nuclear spins in aqueous solution. Hyper-CEST enables nM-to-fM detection of molecules capable of transiently encapsulating xenon.[32–41] Herein, we report TEM-1 β-lactamase as a ^{129}Xe NMR-based PCA reporter, which gives "turn-on" hyper-CEST signal upon assembly of the TEM-1 fragments, T1Fα and T1Fω. TEM-1 assembly was driven by the well-characterized cFos/cJun leucine zipper PPI,[42] which was determined to be readily detectable in bacterial cells.

TEM-1 β-lactamase has been one of the most used PCA reporters since the identification of its α and ω fragments.[2,3] The enzymatic activity of TEM-1 can be used as a proxy to monitor the interaction of the two fusion proteins.[2,43] In some studies, enzymatic activity can be monitored by the conversion of substrate into colorimetric or fluorescent products.[13,44] Moreover, our laboratory previously found that TEM-1 can function as a genetically encoded reporter for ^{129}Xe hyper-CEST NMR.[45] Notably, ^{129}Xe exchanging between TEM-1 and aqueous solvent gives rise to a hyper-CEST signal at +60 ppm, referenced to the ^{129}Xe@aq signal. X-ray crystallography, molecular dynamics (MD) simulations, and protein mutagenesis established the Xe binding site responsible for generating CEST contrast from wild-type TEM-1, which coincidentally resides at the interface between the α and ω fragments of split TEM-1 (Fig. 1).[45,46] We therefore ventured that CEST contrast could be used to monitor PPIs in a turn-on manner using TEM-1 fragment complementation. To investigate this method, we used the α and ω TEM-1 fragments employed by Wehrman *et al.*[3] and

Department of Chemistry, University of Pennsylvania, Philadelphia, Pennsylvania 19104, USA. E-mail: ivandmo@sas.upenn.edu

† Electronic supplementary information (ESI) available: Experimental procedures, sample characterizations and hyper-CEST data. See DOI: 10.1039/d0cc02988b

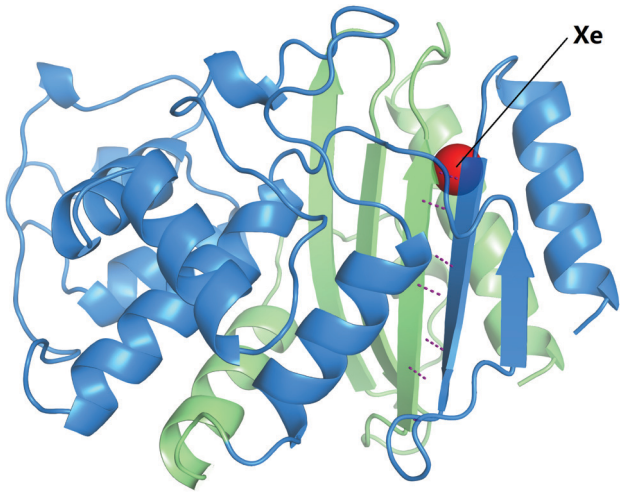

Fig. 1 T1Fα (blue; residues 26–197) and T1Fω fragments (green; residues 198–290) indicated for the crystal structure of TEM-1 derivatized with Xe (PDB ID 5HW1). For simplicity, only the primary xenon site is shown (red atom). Hydrogen bonds between the backbones of the two β-strands at the interface are shown as purple dashed lines.

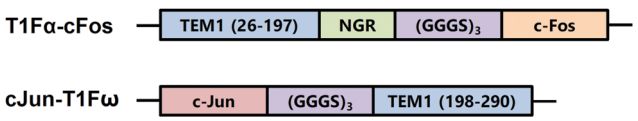

Scheme 1 TEM-1 β-lactamase fragment constructs used in this study.

fused them to complementary cFos and cJun sequences, respectively (T1Fα-cFos and cJun-T1Fω; Scheme 1). Purity and secondary structures of TEM-1 fragments were confirmed by gel electrophoresis and circular dichroism spectroscopy, respectively (Fig. S1 and S2, ESI†). All protein samples remained well-dispersed (non-aggregated) before and after hyper-CEST experiments, as confirmed by dynamic light scattering (Fig. S3, ESI†).

Hyper-CEST *z*-spectra of 80 μM purified recombinant T1Fα-cFos and cJun-T1Fω were obtained using multiple selective d-SNOB saturation pulses (Fig. 2). In the presence of only one

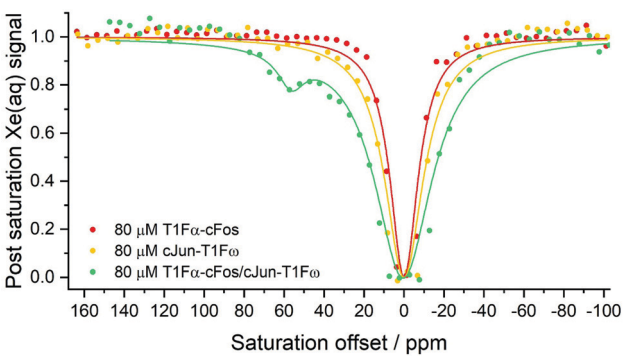

Fig. 2 Hyper-CEST *z*-spectra of 80 μM T1Fα-cFos, 80 μM cJun-T1Fω and 80 μM both fragments in 50 mM Tris (pH 7.4), 500 mM NaCl at 300 K. Saturation time, t_{sat} = 2.29 s; field strength, $B_{1,max}$ = 77 μT. The solid circles show the experimental data, and the lines show the Lorentzian fits. Each spectrum is the average of three measurements.

protein fragment, no ^{129}Xe@protein signal was observable, indicating lack of a site compatible with Xe exchange. In contrast, a sample containing both fragments at equimolar concentration showed a saturation peak at +56 ppm, very close to the chemical shift of ^{129}Xe@wtTEM-1. This suggested that hetero-dimerization of T1Fα-cFos/cJun-T1Fω resembled the protein structure and Xe binding site of wild-type TEM-1. The small difference in chemical shift is likely modulated by slight changes to the protein dynamics and by the presence of cFos/cJun. Notably, the ^{129}Xe@T1Fα-cFos/cJun-T1Fω signal arose from assembly of the two fragments, thereby excluding non-specific protein binding that sometimes can give false signal in enzymatic activity or spectrophotometric assays. The magnitude of the CEST effect ($1 - M_z/M_0 = 0.22$) was attenuated compared to wild-type TEM-1 ($1 - M_z/M_0 = 0.62$),[45] which is likely due to faster Xe exchange and weaker Xe binding affinity as a result of greater protein dynamics and altered topology of split TEM-1. Homo-dimerization of cFos and cJun proteins may also play a role at high micromolar concentrations.[47,48]

To evaluate the detection sensitivity, time-dependent saturation transfer experiments were performed by measuring the ^{129}Xe(aq) signal against varying saturation time using saturation pulses centered at frequency offsets of +56 ppm and −56 ppm, for on- and off-resonance, respectively. T1Fα-cFos/cJun-T1Fω complex (1 μM) gave rise to 0.06 ± 0.01 saturation contrast (Fig. S4, ESI†). To verify that the observed contrast was dependent on the interaction of cFos and cJun, the T1Fα fragment was prepared without the C-terminal cFos and mixed with equimolar cJun-T1Fω fragment. As expected, 1 μM T1Fα/cJun-T1Fω showed minimal background signal with saturation contrast of 0.01 ± 0.01 (Fig. S4, ESI†). This indicated that the limit of detection (LOD) for cFos/cJun PPI was roughly 1 μM. Given that the binding affinity between cFos and cJun is at high nanomolar level,[48] the signal-to-noise ratio and LOD should improve somewhat for stronger protein–protein interactions. The result also indicates that this TEM-1-based approach is useful to probe PPIs with medium to strong affinity (dissociation constant, $K_d < 1$ μM). For weak PPIs ($K_d > 10$ μM), reporter concentration higher than K_d is required for detection.

To investigate the possibility that weak interaction between T1Fα and T1Fω may contribute to background signal at high concentrations, we carried out hyper-CEST experiments with the cFos deletion construct at a concentration of 80 μM. A *z*-spectrum of 80 μM T1Fα/cJun-T1Fω using 77 μT saturation pulses showed a saturation response at +48 ppm somewhat similar to that of T1Fα-cFos/cJun-T1Fω, indicating reconstitution of TEM-1 (Fig. S5, ESI†). This probably results from increased thermostability due to several hydrogen bonds between β-strands at the interface of the two fragments and a reduction of hydrophobic surface area (Fig. 1). Meanwhile, cFos deletion caused a broader peak width of the ^{129}Xe NMR signal, implying faster ^{129}Xe exchange and greater protein dynamics. Time-dependent saturation transfer experiments using 279 μT saturation pulses confirmed that 80 μM T1Fα/cJun-T1Fω gave rise to the same saturation contrast as T1Fα-cFos/cJun-T1Fω (0.44 ± 0.02 and 0.42 ± 0.02, respectively; Fig. S6, ESI†).

Table 1 Hyper-CEST data for *E. coli* samples expressing TEM-1 fragments

E. coli sample	$T_{1,on}$/s	$T_{1,off}$/s	Saturation contrast
T1Fα-cFos/cJun-T1Fω, non-induced	16.0 ± 0.6	19.0 ± 0.7	0.10 ± 0.02
T1Fα-cFos/cJun-T1Fω, induced	16.0 ± 0.6	21.7 ± 0.7	0.18 ± 0.02
T1Fα/cJun-T1Fω, non-induced	14.1 ± 0.6	16.8 ± 0.3	0.12 ± 0.02
T1Fα/cJun-T1Fω, induced	17.1 ± 0.5	21.3 ± 0.6	0.12 ± 0.02

As non-specific Xe–protein interactions sometimes contribute to saturation contrast, especially at a high pulse power setting, *z*-spectra of 80 μM protein samples using 279 μT saturation pulses were acquired and confirmed that the observed saturation contrast at this high pulse power is indeed due to interaction of the two fragments (Fig. S7, ESI†). Thus, regardless of fusion protein interactions, split TEM-1 has the potential to give background signal. This background was recognized in previous studies but thought to be negligible considering the high signal-to-noise ratio.[2,3] Our results provide a cautionary note, showing that under conditions with high protein concentration (80 μM), the background signal resulting from spontaneous complementation makes split TEM-1 unsuitable for monitoring PPIs. This opens possibilities for engineering the split protein complementation reporter for studying weak PPIs.[8]

The hyper-CEST saturation contrast was then assessed in a cellular environment. *E. coli* strain BL21(DE3) cells co-expressing α and ω fragments were cultured in LB media, induced with isopropyl β-D-1-thiogalactopyranoside (IPTG), resuspended in PBS to an OD_{600} of 1, and tested by time-dependent saturation transfer experiments (Table 1 and Fig. S8, ESI†). Serving as negative controls, cells co-expressing the T1Fα/cJun-T1Fω pair with and without IPTG induction both reported saturation contrast of 0.12 ± 0.02 at +56 ppm. Similar background contrast was observed previously to originate from the nonspecific interaction of Xe with intracellular biomacromolecules.[45,49–52] *E. coli* cells co-expressing the interacting pair T1Fα-cFos/cJun-T1Fω showed saturation contrast of 0.18 ± 0.02 and 0.10 ± 0.02, with and without IPTG induction, respectively. The cFos/cJun interaction in *E. coli* cells reported saturation contrast of 0.08 after subtracting the non-induced background signal, and cFos deletion samples showed no change in saturation contrast, highlighting that ^{129}Xe NMR can readily detect PPIs in bacterial cells.

TEM-1 β-lactamase is non-toxic to prokaryotic and eukaryotic cells, and no orthologs of TEM-1 exist in eukaryotes. Therefore, the TEM-1-based complementation assay could be universally used in eukaryotic cells and many prokaryotes without intrinsic background activity. The ability of reconstituted (split) TEM-1 to bind xenon and report PPIs *in vitro* and *in vivo* using sensitive and selective hyper-CEST ^{129}Xe NMR spectroscopy can expand the range of applications of PCAs in various biological systems. However, modest affinity between T1Fα and T1Fω fragments can result in background signal at high micromolar protein concentrations. It should be possible to reduce the intrinsic T1Fα/T1Fω interaction by disrupting several hydrogen bonds and salt bridges between T1Fα and T1Fω, which also has the potential to modulate Xe affinity. In enzymatic activity assays, the signal-to-noise ratio was improved by up to 10^4-fold *via* optimization of side chain contacts with the active site of TEM-1.[3] Likewise, we envision that mutating Xe binding site residues can give enhancement to saturation contrast, as was previously demonstrated for maltose binding protein.[49] Significant signal enhancement can also be achieved by use of isotopically enriched ^{129}Xe and/or higher ^{129}Xe hyperpolarization levels.[53] Finally, the TEM-1 fragment complementation assay also holds promise for molecular recognition and selective turn-on sensing using ^{129}Xe NMR/MRI, which has been a challenging task.[49,54–57]

We thank the University of Pennsylvania Chemistry NMR facility for spectrometer time. This work was supported by NIH grant R35-GM-131907.

Conflicts of interest

There are no conflicts to declare.

Notes and references

1 T. K. Kerppola, *Nat. Methods*, 2006, **3**, 969–971.
2 A. Galarneau, M. Primeau, L. E. Trudeau and S. W. Michnick, *Nat. Biotechnol.*, 2002, **20**, 619–622.
3 T. Wehrman, B. Kleaveland, J. H. Her, R. F. Balint and H. M. Blau, *Proc. Natl. Acad. Sci. U. S. A.*, 2002, **99**, 3469–3474.
4 I. Ghosh, A. D. Hamilton and L. Regan, *J. Am. Chem. Soc.*, 2000, **122**, 5658–5659.
5 R. Paulmurugan and S. S. Gambhir, *Anal. Chem.*, 2005, **77**, 1295–1302.
6 R. Paulmurugan, Y. Umezawa and S. S. Gambhir, *Proc. Natl. Acad. Sci. U. S. A.*, 2002, **99**, 15608–15613.
7 J. N. Pelletier, F. X. Campbell-Valois and S. W. Michnick, *Proc. Natl. Acad. Sci. U. S. A.*, 1998, **95**, 12141–12146.
8 A. S. Dixon, M. K. Schwinn, M. P. Hall, K. Zimmerman, P. Otto, T. H. Lubben, B. L. Butler, B. F. Binkowski, T. Machleidt, T. A. Kirkland, M. G. Wood, C. T. Eggers, L. P. Encell and K. V. Wood, *ACS Chem. Biol.*, 2016, **11**, 400–408.
9 G. S. Loving, M. Sainlos and B. Imperiali, *Trends Biotechnol.*, 2010, **28**, 73–83.
10 T. K. Kerppola, *Chem. Soc. Rev.*, 2009, **38**, 2876–2886.
11 X. Dai, M. Zhu and Y. P. Wang, *Chem. Commun.*, 2014, **50**, 1830–1832.
12 T. Kakizuka, A. Takai, K. Yoshizawa, Y. Okada and T. M. Watanabe, *Chem. Commun.*, 2020, **56**, 3625–3628.
13 I. Remy, G. Ghaddar and S. W. Michnick, *Nat. Protoc.*, 2007, **2**, 2302–2306.
14 E. Tchekanda, D. Sivanesan and S. W. Michnick, *Nat. Methods*, 2014, **11**, 641–644.
15 B. R. Sculimbrene and B. Imperiali, *J. Am. Chem. Soc.*, 2006, **128**, 7346–7352.
16 E. Stefan, S. Aquin, N. Berger, C. R. Landry, B. Nyfeler, M. Bouvier and S. W. Michnick, *Proc. Natl. Acad. Sci. U. S. A.*, 2007, **104**, 16916–16921.
17 G. Loving and B. Imperiali, *J. Am. Chem. Soc.*, 2008, **130**, 13630–13638.
18 I. A. Demarco, A. Periasamy, C. F. Booker and R. N. Day, *Nat. Methods*, 2006, **3**, 519–524.
19 I. Remy and S. W. Michnick, *Nat. Methods*, 2006, **3**, 977–979.
20 C. D. Hu and T. K. Kerppola, *Nat. Biotechnol.*, 2003, **21**, 539–545.
21 S. A. Slavoff, D. S. Liu, J. D. Cohen and A. Y. Ting, *J. Am. Chem. Soc.*, 2011, **133**, 19769–19776.
22 E. Barile and M. Pellecchia, *Chem. Rev.*, 2014, **114**, 4749–4763.
23 E. R. Zuiderweg, *Biochemistry*, 2002, **41**, 1–7.
24 L. D'Silva, P. Ozdowy, M. Krajewski, U. Rothweiler, M. Singh and T. A. Holak, *J. Am. Chem. Soc.*, 2005, **127**, 13220–13226.
25 A. M. Bonvin, R. Boelens and R. Kaptein, *Curr. Opin. Chem. Biol.*, 2005, **9**, 501–508.
26 D. S. Burz, K. Dutta, D. Cowburn and A. Shekhtman, *Nat. Methods*, 2006, **3**, 91–93.

27 M. P. Williamson, *Prog. Nucl. Magn. Reson. Spectrosc.*, 2013, **73**, 1–16.
28 M. L. Ludwiczek, B. Baminger and R. Konrat, *J. Am. Chem. Soc.*, 2004, **126**, 1636–1637.
29 M. Somlyay, K. Ledolter, M. Kitzler, G. Sandford, S. L. Cobb and R. Konrat, *ChemBioChem*, 2020, **21**, 696–701.
30 P. Raffeiner, A. Schraffl, T. Schwarz, R. Rock, K. Ledolter, M. Hartl, R. Konrat, E. Stefan and K. Bister, *Oncotarget*, 2017, **8**, 3327–3343.
31 L. Schröder, T. J. Lowery, C. Hilty, D. E. Wemmer and A. Pines, *Science*, 2006, **314**, 446–449.
32 Y. Bai, P. A. Hill and I. J. Dmochowski, *Anal. Chem.*, 2012, **84**, 9935–9941.
33 Y. Wang and I. J. Dmochowski, *Chem. Commun.*, 2015, **51**, 8982–8985.
34 M. G. Shapiro, R. M. Ramirez, L. J. Sperling, G. Sun, J. Sun, A. Pines, D. V. Schaffer and V. S. Bajaj, *Nat. Chem.*, 2014, **6**, 629–634.
35 T. K. Stevens, K. K. Palaniappan, R. M. Ramirez, M. B. Francis, D. E. Wemmer and A. Pines, *Magn. Reson. Med.*, 2013, **69**, 1245–1252.
36 T. K. Stevens, R. M. Ramirez and A. Pines, *J. Am. Chem. Soc.*, 2013, **135**, 9576–9579.
37 T. Meldrum, K. L. Seim, V. S. Bajaj, K. K. Palaniappan, W. Wu, M. B. Francis, D. E. Wemmer and A. Pines, *J. Am. Chem. Soc.*, 2010, **132**, 5936–5937.
38 L. Schröder, T. Meldrum, M. Smith, T. J. Lowery, D. E. Wemmer and A. Pines, *Phys. Rev. Lett.*, 2008, **100**, 257603.
39 H. M. Rose, C. Witte, F. Rossella, S. Klippel, C. Freund and L. Schröder, *Proc. Natl. Acad. Sci. U. S. A.*, 2014, **111**, 11697–11702.
40 M. Kunth, J. Dopfert, C. Witte, F. Rossella and L. Schröder, *Angew. Chem., Int. Ed.*, 2012, **51**, 8217–8220.
41 M. Schnurr, K. Sydow, H. M. Rose, M. Dathe and L. Schröder, *Adv. Healthcare Mater.*, 2015, **4**, 40–45.
42 L. J. Ransone, J. Visvader, P. Sassonecorsi and I. M. Verma, *Genes Dev.*, 1989, **3**, 770–781.
43 J. C. Saunders, L. M. Young, R. A. Mahood, M. P. Jackson, C. H. Revill, R. J. Foster, D. A. Smith, A. E. Ashcroft, D. J. Brockwell and S. E. Radford, *Nat. Chem. Biol.*, 2016, **12**, 94–101.
44 C. K. Zhao, Q. Yin and S. Y. Li, *Acta Pharmacol. Sin.*, 2010, **31**, 1618–1624.
45 Y. Wang, B. W. Roose, E. J. Palovcak, V. Carnevale and I. J. Dmochowski, *Angew. Chem., Int. Ed.*, 2016, **55**, 8984–8987.
46 B. W. Roose, S. D. Zemerov, Y. Wang, M. A. Kasimova, V. Carnevale and I. J. Dmochowski, *ChemPhysChem*, 2019, **20**, 260–267.
47 T. D. Halazonetis, K. Georgopoulos, M. E. Greenberg and P. Leder, *Cell*, 1988, **55**, 917–924.
48 N. Szaloki, J. W. Krieger, I. Komaromi, K. Toth and G. Vamosi, *Mol. Cell. Biol.*, 2015, **35**, 3785–3798.
49 B. W. Roose, S. D. Zemerov and I. J. Dmochowski, *Chem. Sci.*, 2017, **8**, 7631–7636.
50 C. Boutin, H. Desvaux, M. Carriere, F. Leteurtre, N. Jamin, Y. Boulard and P. Berthault, *NMR Biomed.*, 2011, **24**, 1264–1269.
51 K. K. Palaniappan, R. M. Ramirez, V. S. Bajaj, D. E. Wemmer, A. Pines and M. B. Francis, *Angew. Chem., Int. Ed.*, 2013, **52**, 4849–4853.
52 A. Bifone, Y. Q. Song, R. Seydoux, R. E. Taylor, B. M. Goodson, T. Pietrass, T. F. Budinger, G. Navon and A. Pines, *Proc. Natl. Acad. Sci. U. S. A.*, 1996, **93**, 12932–12936.
53 P. Nikolaou, A. M. Coffey, L. L. Walkup, B. M. Gust, N. Whiting, H. Newton, S. Barcus, I. Muradyan, M. Dabaghyan, G. D. Moroz, M. S. Rosen, S. Patz, M. J. Barlow, E. Y. Chekmenev and B. M. Goodson, *Proc. Natl. Acad. Sci. U. S. A.*, 2013, **110**, 14150–14155.
54 C. C. Slack, J. A. Finbloom, K. Jeong, C. J. Bruns, D. E. Wemmer, A. Pines and M. B. Francis, *Chem. Commun.*, 2017, **53**, 1076–1079.
55 J. A. Finbloom, C. C. Slack, C. J. Bruns, K. Jeong, D. E. Wemmer, A. Pines and M. B. Francis, *Chem. Commun.*, 2016, **52**, 3119–3122.
56 N. Kotera, N. Tassali, E. Leonce, C. Boutin, P. Berthault, T. Brotin, J. P. Dutasta, L. Delacour, T. Traore, D. A. Buisson, F. Taran, S. Coudert and B. Rousseau, *Angew. Chem., Int. Ed.*, 2012, **51**, 4100–4103.
57 N. Tassali, N. Kotera, C. Boutin, E. Leonce, Y. Boulard, B. Rousseau, E. Dubost, F. Taran, T. Brotin, J. P. Dutasta and P. Berthault, *Anal. Chem.*, 2014, **86**, 1783–1788.